Journal of Hydrology 612 (2022) 128178

Contents lists available at ScienceDirect

Journal of Hydrology

journal homepage: www.elsevier.com/locate/jhydrol

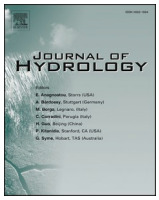

Research papers

Catchment scale effects of low impact development implementation scenarios at different urbanization densities

Ninon Le Floch [a], Vincent Pons [a,b,*], Elhadi Mohsen Hassan Abdalla [a], Knut Alfredsen [a]

[a] Department of Civil and Environmental Engineering, Norwegian University of Science and Technology, Andersens vei 5, Trondelag 7031, Norway
[b] Univ. Lyon, INSA Lyon, DEEP, EA7429, 11 rue de la Physique, 69621, Villeurbanne Cedex, France

ARTICLE INFO

Keywords:
Low Impact Development
LID implementation scenarios
Climate change adaptation
SWMM
Sensitivity analysis

ABSTRACT

Climate change and urbanization put stress on urban stormwater systems, triggering hydraulic overloading and urban flooding increase. Low Impact Development (LID) techniques have a high potential to mitigate their impacts. This study investigates the consequences of climate change and urbanization on the urban runoff in the Risvollan catchment in Trondheim, Norway, and the effects of LID implementation and the influence of LID spatial distributions on their performance. A SWMM model of Risvollan was implemented, along with different scenarios of urbanization and climate change. The performance of various spatial distributions of LID infrastructures in the catchment was investigated, using the outflow volume and the peak runoff at the outfall as indicators. The rainfall event-based simulation results confirmed the negative effects of urbanization and climate change on urban runoff. These effects were partially mitigated by a homogenous LID implementation. The different spatial distributions of LID had little impact on volume reduction but targeting the most downstream zones of the model was more efficient in reducing the peaks at the catchment's outlet. These findings confirm that the spatial configuration of LID might be a determinant parameter towards an efficient design of LID infrastructure in urban settings, depending on the local stakes and criteria of urban water management.

1. Introduction

In Norway, rainfall intensity and amount are expected to increase in the future due to climate change (Sorteberg et al., 2018). On the other hand, urbanization alters runoff formation by sealing permeable surfaces, thus limiting infiltration and evaporation of water (Shuster et al., 2005) and increasing stormwater runoff. The combined effect of climate change and rapid urbanization will increase the volume and intensity of stormwater in the future. Consequently, many stormwater management systems are at risk of increased overflow frequency, with the associated urban flooding and sewage overflow (Skougaard Kaspersen et al., 2017), which will have significant economic (Zhou et al., 2012), health (Han & He, 2021) and environmental (Semadeni-Davies et al., 2008) consequences.

In the last few decades, low-impact development (LID) infrastructures have been regarded as sustainable stormwater solutions that mitigate climate change and rapid urbanization. LID techniques increase permeability and vegetation cover of urban catchments, which enhance evapotranspiration and infiltration and reduce the amount of stormwater runoff flowing to the drainage network (Eckart et al., 2017). Among the LID infrastructures, green roofs and permeable pavements have the potential to reduce stormwater volumes permanently. Additionally, they attenuate and delay the drainage outflows due to water's temporal storage and routing, which is beneficial for stormwater management.

For green roofs, volume reduction due to evapotranspiration was found to vary between 11 and 59 % of the annual precipitation in cold and wet climatic regions (Bengtsson et al., 2005; Johannessen et al., 2018; Stovin, 2010). Furthermore, green roofs were found to attenuate drainage outflows by 59–90 % (Johannessen et al., 2018; Palla et al., 2011; Stovin et al., 2012). These are significant figures for stormwater management, considering that building roofs account for up to 50 % of impervious areas in densely urbanized catchments (Dunnett & Kingsbury, 2004). On the other hand, permeable pavements provide high volume reduction due to infiltration (Drake et al., 2013). Significant volume reduction can also be obtained even when permeable pavements are constructed over soils with low permeability (Dreelin et al., 2006). Furthermore, permeable pavements were found to detain the drainage

* Corresponding author at: Department of Civil and Environmental Engineering, Norwegian University of Science and Technology, Andersens vei 5, Trondelag 7031, Norway.
E-mail address: vincent.pons@ntnu.no (V. Pons).

https://doi.org/10.1016/j.jhydrol.2022.128178
Received 5 January 2022; Received in revised form 22 April 2022; Accepted 4 July 2022
Available online 19 July 2022

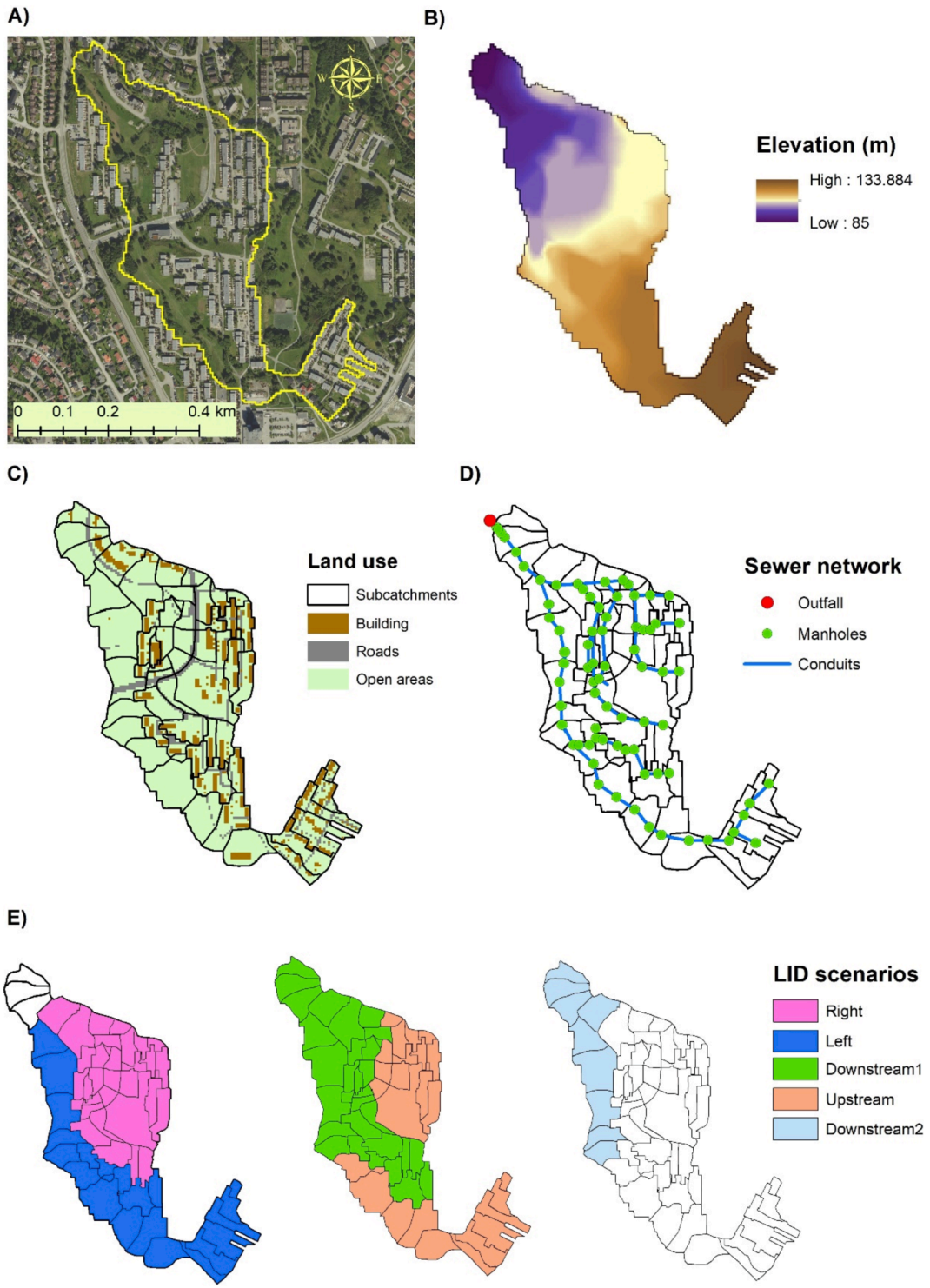

Fig. 1. A) Orthophoto of Risvollan catchment (© Statens kartverk, Geovekst and Trondheim municipality). B) Digital elevation model of Risvollan. C) Land use of Risvollan. D) Sewer network of Risvollan. E) Catchment zones for LID implementation scenarios.

flow effectively with an average peak reduction of around 80 % (Braswell et al., 2018; Winston et al., 2018) and average peak delay between 15 mins to 4 h (Fassman & Blackbourn, 2010; Støvring et al., 2018).

Numerous studies have investigated the catchment-scale implementation of LID infrastructure to identify the density of LID measures needed to achieve desirable hydrological performances. For instance, Palla & Gnecco (2015) concluded that at least 5 % of impervious surfaces should be converted into LID measures to obtain noticeable hydrological benefits at the catchment scale. Hamouz et al. (2020) stated that retrofitting 11 % of the building with green roofs would substantially reduce the maximum flow at the catchment outlet. Hernes et al. (2020) presented the effect of different LID densities on the resulting combined sewer overflow at the catchment outlet. Skaugen et al. (2020) concluded that for their study case, an urban catchment with 500 houses, 60 rain gardens (unit area of 10 m^2) are needed to reduce the peak flow by 10 %.

Recently, the spatial configuration of LID measures in urban catchments has been regarded as an impactful parameter for the efficiency of

stormwater management at the catchment scale (Giacomoni & Joseph, 2017). However, only a few studies have been found to investigate this topic. For instance, Yao et al. (2020) examined different spatial configurations of green roofs and found that retrofitting roofs directly connected to the drainage network achieves higher hydrological benefits. Likewise, Liang et al. (2020) concluded that a higher peak reduction could be achieved at the catchment outlet by implementing LID measures in areas directly connected to the drainage network. Hou et al. (2020) found that placing LID measures near areas sensitive to flooding and pollution is the most cost-effective strategy. Similarly, Ercolani et al. (2018) recommend placing LID measures near portions of the drainage network that are prone to overflowing. Giacomoni & Joseph (2017) found placing LID measures at the downstream portion of the catchment to yield better peak reduction at the outlet while placing LID measures at the upstream reduces the surface flooding at the downstream areas.

Hydrological models are essential tools for studies that aim to evaluate LID implementation scenarios at the catchment scale. The EPA's Storm Water Management Model (SWMM) is perhaps the most common tool for these studies. However, most of these studies applied SWMM catchment models without calibration (Liang et al., 2020; Yao et al., 2020). Indeed, this is a limitation as uncalibrated SWMM models might yield unsatisfactory modelling performances (Peng & Stovin, 2017), which could alter the findings of such studies. On the other hand, many scholars have attempted to calibrate SWMM catchment models by altering physical properties such as the percentage of imperviousness (Hamouz et al., 2020). This practice is questionable since LID implementation scenarios would also involve changing the degree of imperviousness and hence abolishing the calibration setup. There is a clear need for a proper sensitivity analysis to identify the most influential SWMM catchment model parameters for calibration without changing the physical properties, such as the degree of imperviousness.

The motivation for this study was to investigate the influence of the spatial distribution and density of LID measures on runoff mitigation and provide insights to improve the robustness of implementation strategies of LID infrastructures within an urban catchment. This work implemented the SWMM model for an urban catchment in Trondheim, Norway, and several urbanizations and climate change scenarios. LID techniques integration at different spatial locations and densities was also implemented. This paper addresses the following:

(i) Identification of the most sensitive parameters of the SWMM modelling approach
(ii) Modelling of the combined impact of climate change and urbanization on runoff mitigation
(iii) Comparison of different spatial configurations for LID implementation.

2. Methods

2.1. Study site and data

The study area is an urban catchment, Risvollan, in Trondheim city, Norway. A separate stormwater management system drains water over 20.6 ha in the residential area of Risvollan, in the south-east of the city, where the elevation varies between 85 and 134 m.a.s.l. This study used the GIS spatial data, subcatchments delineation and stormwater network data from Hailegeorgis & Alfredsen (2018) study. The catchment was considered 27 % impervious area, with 14 % roofs, 9 % roads and 4 % sidewalks, and 73 % pervious area, including grasslands, vegetated areas, and some built-up zones. Most of the land cover delineations were done using aerial photos and local land use maps, while the sidewalk areas were obtained by 1 m buffering around the road zones. The catchment was subdivided into 55 subcatchments, on average of 0.39 ha, linked together by a stormwater network comprised of 78 manholes, 78 conduits and one outlet. Fig. 1 presents a map of the area, including subcatchment delineation, land cover delineation and an outline of the stormwater network. A measure station next to the outlet provides several decades of 1-min precipitation and temperature data. Precipitation was measured with an unshielded Lambrecht tipping bucket, with 0.1 mm per tip. Stormwater flow data at the outfall of the catchment was also collected with a 1-min resolution. Missing stormwater flow data was interpolated linearly, and time periods with significant missing data were excluded from the study.

2.2. Model and model setup

The study system and area are modelled in the EPA's Storm Water Management Model (SWMM), an open-source model first developed in 1971, and widely used for planning, design, and analysis of stormwater systems. This study used the version 5.1 that incorporates LID modelling for various types of green infrastructure, such as green roofs and permeable pavements (Rossman, 2015). The model set-up from GIS data, as well as all future manipulations for calibration, sensitivity study and scenarios exploration, were done in R programming language using the swmmr package (Leutnant et al., 2019). In this study, the SWMM catchment model simulates the rainfall/runoff process using the Green-Ampt equation for infiltration and kinematic wave formula for runoff routing (Rossman, 2015). All simulations were event-based. Hence, evaporation was ignored in this study.

Both permeable pavements and green roofs were implemented in this study, using the internal LID module in SWMM (Rossman, 2015). This module simulates the hydrological processes of green roofs using Green-Ampt equation for surface infiltration to the soil layer, Darcy's equation for percolation to the drainage layer and manning formula for drainage layer outflow. For permeable pavement, the water infiltrates from the surface directly to the soil layer (the bedding layer), limited by the permeability of the surface layer. The percolation from the bedding layer to the base layer is determined following Darcy's equations, and the drainage flow is determined by an empirical power equation (Rossman, 2015).

The green roof type implemented consisted of a 30 mm vegetation mat over a 10 mm textile retention fabric and was designed for sloped roofs. All green roofs implemented had the same unit area of 15 m^2 and the same unit width of 7.5 m. Their parameters for the surface, soil and drainage layers in the SWMM model were obtained from Johannessen et al. (2019). A permeable pavement with a bottom liner was implemented in the study. It comprises of an interlocking pavement of 80 mm thickness with 10 mm joints that allows water to infiltrate into a 30 mm bedding layer. The base layer was 100 mm thick and made of coarse materials, and the subbase layer was 250 mm thick. The pavement was lined with an impermeable geotextile. All permeable pavements implemented had the same unit area of 100 m^2 and the same unit width of 8 m. The parameters for the SWMM implementation of the permeable pavements were obtained from Abdalla et al. (2021).

2.3. Calibration and validation

Rainfall-runoff events were extracted for calibration and validation from the precipitation and the stormwater runoff data of the recent years (2016 to 2019) to account for recent urbanization and land use change in the catchment. The start of events was defined at the first rainfall measurement, and the end was defined when the flow returns to the minimum measured value of 0.001 m^3/s. To eliminate too small events, only those with an accumulated precipitation greater than 3 mm were considered. This yielded several dozens of events for the four years.

The physical model parameters, such as subcatchment width, area, slope, imperviousness degree, as well as manholes and pipes geometric characteristics, were extracted from Hailegeorgis & Alfredsen, (2018) study. In their study, they developed a distributed hydrological model for the Risvollan catchment with high spatial resolution to account for variability of land use and land cover of the catchment. They found a grid size of 5 × 5 m to be sufficient for accounting for the spatial

Table 1
SWMM parameters selected for calibration, their selected ranges and optimal ranges of the ensemble.

	Parameter	Abbreviated name	Unit	Lower Bound	Upper bound	ensemble range
Infiltration in pervious subcatchments	Hydraulic conductivity in pervious zones	$Ksat_{Per}$	mm/h	0.1	10	0.08–3.27
	Initial moisture deficit in pervious zones	$IniMoistDef_{Per}$	–	0	1	0–1
	Suction head in pervious zones	$Suction_{Per}$	mm/h	0.1	10	0.89–9.5
Infiltration in impervious subcatchments	Hydraulic conductivity in impervious zones	$Ksat_{Imp}$	mm/h	0.1	10	0.15–5.31
	Initial moisture deficit in impervious zones	$IniMoistDef_{Imp}$	–	0	1	0–1
	Suction head in impervious zones	$Suction_{Imp}$	mm/h	0.1	10	4.07–9.78
Common to all subcatchments	Depression storage in impervious zones	$DepSto_{Imp}$	mm	0.01	1	0.98
	Depression storage in pervious zones	$DepSto_{Per}$	mm	0.01	1	0.95
	Manning's pipe roughness	*Roughness*	$s.m^{-\frac{1}{3}}$	0.01	0.5	0.15–0.34
	Seepage rate	*Seepage*	mm/h	0	250	1.53–97
	Baseflow	*BasFlow*	L/s	0	0.8	0.05–0.32

Table 2
Summary of extracted rainfall events.

	Event name	Start date and time	End date and time	Duration (h)	Peak (mm/min)	Amount (mm)	Return period (years)
Calibration events	C_1	29.09.2016 23:07	30.09.2016 07:23	8.27	0.2	10.3	<1
	C_2	10.08.2018 09:37	11.08.2018 20:22	34.75	0.3	40.6	<1
	C_3	19.08.2017 13:27	21.08.2017 13:06	47.65	0.5	46.6	<1
	C_4	27.10.2017 19:10	30.10.2017 11:06	64.93	0.2	37.4	<1
	C_5	30.10.2019 15:26	02.11.2019 01:13	57.78	0.2	17.5	<1
	C_6	13.09.2019 09:22	22.09.2019 12:13	218.85	0.4	107	<1
	C_7	30.10.2017 15:40	03.11.2017 09:17	89.62	0.1	27.7	<1
Validation events	V_1	29.08.2019 13:54	29.08.2019 19:37	5.72	0.4	8.6	<1
	V_2	07.06.2019 10:39	07.06.2019 18:08	7.48	0.3	8.9	<1
	V_3	11.07.2017 23:58	12.07.2017 09:45	9.78	0.2	7.9	<1
	V_4	18.10.2017 02:59	18.10.2017 15:20	12.35	0.3	6.1	<1
	V_5	18.06.2017 18:39	22.06.2017 05:36	46.63	0.2	34.1	<1
	V_6	22.09.2018 11:25	02.10.2018 18:13	5.07	0.2	98.5	<1
	V_7	18.04.2018 02:03	23.04.2018 07:58	64.93	0.6	17.5	<1
Rainfall events for scenarios analysis	E_1	20.07.2009 00:00	20.07.2009 23:59	24	0.2	68.9	20
	E_2	29.07.2007 00:00	29.07.2007 12:00	12.00	1	42.5	5
	E_3	05.06.2003 12:59	05.06.2003 19:00	6.00	0.7	30.7	5
	E_4	13.08.2007 18:15	13.08.2007 18:45	0.3	3.3	11.8	100

variability. Accordingly, and through GIS analysis, they divided the catchment into 55 subcatchments that are connected with a network of pipes and manholes. Their model achieves satisfactory results, indicating that the spatial discretization was adequate. Therefore, we decided to use the spatial discretization from their study. Another reason to use spatial discretization from Hailegeorgis & Alfredsen, (2018) study is the fact that SWMM is a semi-distributed hydrological model. Hence, spatial discretization with high resolution is needed to analyse and compare different spatial configurations of LID measures at a catchment scale.

The Manning's roughness for the impervious zones was set to 0.013 in impervious zones and 0.15 in pervious zones, in accordance with the values provided in the SWMM User Manual (Rossman, 2015). The subcatchments were divided into two categories, depending on their impervious rate. A threshold of 30 % of imperviousness was selected to separate pervious and impervious subcatchments. This denomination criterion was carried on for the relevant model parameters. It differentiated between the subcatchments containing mainly open grassland and vegetation, and those comprising a more significant part of human constructions and built-up areas.

The calibrated parameters were the parameters of Green Ampt infiltration equation, i.e. saturated hydraulic conductivity and suction head, attributed to each subcatchment category, initial moisture deficit for pervious and impervious sub-catchments,depression storage volumes for both pervious and impervious zones in all subcatchments, the seepage loss rate in the pipe network and Manning's roughness of pipes, as well as the baseflow of the drainage pipes, for a total for 11 calibrated parameters. The baseflow is related to processes that were not included in the model, such as leakage from the drinking water system, and connections to the wastewater system. The boundaries for the infiltration, depression storage and seepage rate were set using the SWMM User Manual (Rossman, 2015), and the baseflow boundaries were set around the minimal measured outflow. The pipe roughness was calibrated outside its recommended range in the SWMM manual to account for model delays and network irregularities (e.g., obstructions, singular energy losses points or unforeseen leakages). The summary of the boundaries for each parameter is visible in Table 1.

The calibration was performed using the Differential Evolution algorithm (Storn & Price, 1997) using the DEoptim library in R (Mullen et al., 2011). Initially, the algorithm creates a population of random solutions by selecting model parameters from given ranges. Each of the solutions is evaluated based on the value of the objective function. Then, the algorithm creates a new population in a way that each solution is either improved or remains the same. This process continues for a number of iterations (100 in this study) and the best solution in the last population is selected as the optimal. The calibration process used Kling-Gupta efficiency KGE as the objective function (Gupta et al., 2009) to evaluate the goodness-of-fit of the modelled output compared to the measurements of outflow.

Seven events were chosen for calibration by excluding winter events and aiming for variety in rainfall hyetograph shapes (Table 2). The time step for modelling was selected as 10 min and hence rainfall and runoff data were aggregated accordingly. The calibration was performed in three steps as follows:

1. One selected event (C_3) was calibrated;

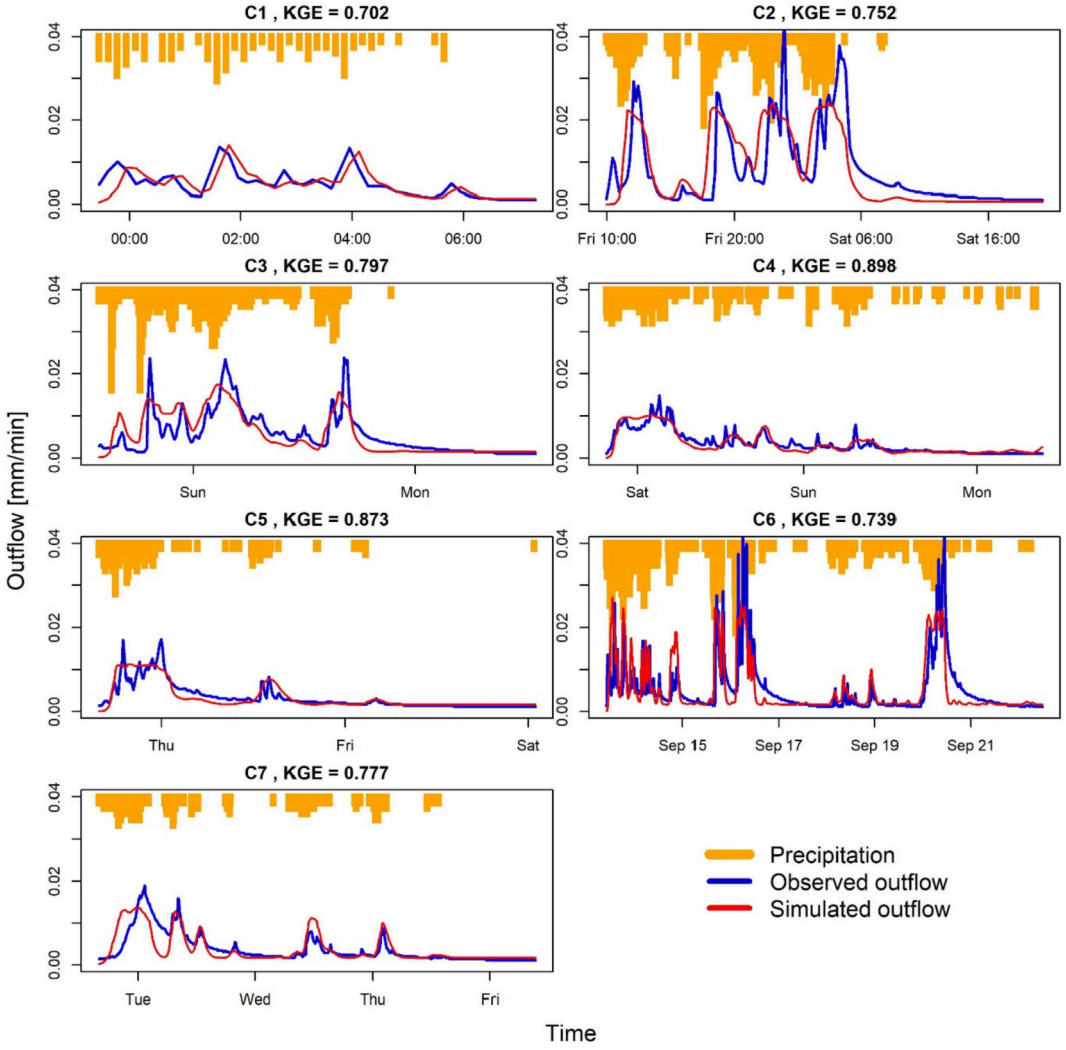

Fig. 2. Calibration results of the SWMM model.

2. The initial soil moisture deficits of each of the seven calibrated events were optimized. This was achieved after fixing all other parameters to the values of the optimal parameter set of C_3;
3. The depression storages are fixed to the optimal value of C_3 and the optimal initial saturation of each event are fixed. Then, the remining model parameters were optimized for each event separately.

This process resulted in a different parameter set for each of the seven calibrated events. These parameter sets were considered for ensemble simulation in which each parameter set yields different flow simulation. The results of ensemble simulations are combined to provide a measure of uncertainty due to model parameters.

Six validation events were extracted from 2016 to 2019 data in the same fashion as the calibration events and are presented in Table 2. The calibrated models of the ensemble were applied to provide flow simulations for those events. The model performance was evaluated against the average of the ensemble using KGE (equation (1)).

$$KGE = 1 - \sqrt{(r-1)^2 + (\alpha-1)^2 + (\beta-1)^2} \quad (1)$$

r is the correlation between simulations and observation, α is the measure of flow variability error and β is the measure of the volumetric error (percentage bias).

2.4. Sensitivity analysis

A sensitivity analysis of the parameters was carried out to screen the parameters of the model. This approach can also constitute a first analysis of the uncertainty of the simulation results.

The applied method was derived from the GLUE methodology (Beven & Binley, 1992), implemented in a similar fashion to Krebs et al. (2016). Also referred to as Monte-Carlo filtering (Saltelli et al., 2007), this method relies on Monte-Carlo simulations with a filtering method to distinguish behavioural and non-behavioural parameter sets. The behavioural parameter sets are defined as parameter sets leading to performance higher than a specific threshold value of the objective function. The initial distribution of parameter sets is considered as a prior while the filtered distribution stand for a posterior distribution. The sensitivity is evaluated by computing the Kolmogorov Smirnov (KS) distance between the prior and posterior distribution of each parameter. The distance associated to each parameter is then screened to select the most behavioural parameter, i.e. the parameters with the largest statistical distance between prior and posterior.

The Sobol sequence (Sobol, 2001) was chosen to sample 65 000 sets of the 11 parameters. The model was run with event C_3 (Table 2) for each of the parameter sets. The performance was evaluated with three objectives functions (equations 1, 2 and 3). The KGE threshold used to separate behavioural and non-behavioural parameters was 0.58. To evaluate the results of the GLUE-based sensitivity screening, the method

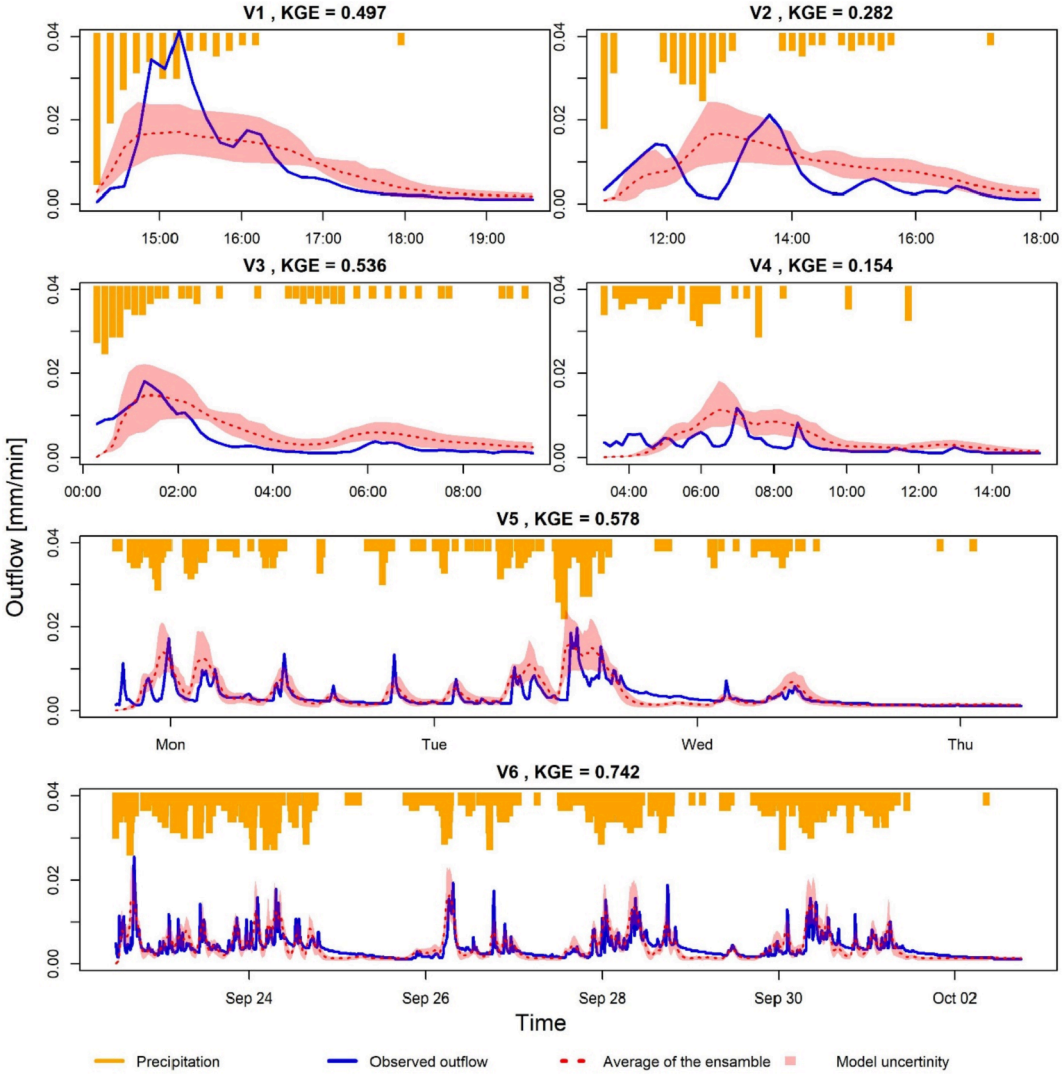

Fig. 3. Validation results of the SWMM model. The shaded areas represent the variabilities within the ensemble.

was confirmed using another sensitivity analysis method, the RBD-FAST method (Random Balance Design – Fourier Amplitude Sensitivity Test) (Tarantola et al., 2006) and Sobol 1st order and total effect indices (Sobol, 2001). For this purpose, the sensitivity analysis was also applied to the KGE, NSE and the PBIAS with GLUE and the RBD-FAST. Different thresholds were chosen for the GLUE methodology to ensure that the filtered dataset include 15 %, 5 % and 1 % of the sampled parameter. In addition, Pearson correlation coefficients were determined between the behavioural parameters to evaluate correlations between model parameters.

$$\mathrm{NSE} = 1 - \frac{\sum (\mathrm{Q_{obs}} - \mathrm{Q_{sim}})^2}{\sum (\mathrm{Q_{obs}} - \overline{\mathrm{Q_{obs}}})^2} \tag{2}$$

$$PBIAS = 100 \times \frac{\sum Q_{sim} - \sum Q_{obs}}{\sum Q_{obs}} \tag{3}$$

Q_{obs} and Q_{sim} are the observed and simulated runoff, respectively.

2.5. Urbanization, climate and LID scenarios

2.5.1. Rainfall-Runoff analysis and runoff descriptors

It has been demonstrated that the performance of green roofs is influenced by the rainfall intensity and shape of the hyetograph (Eckart et al., 2017; Yao et al., 2020). In this work, real recorded rainfall events of different durations were chosen from historical data, with a 1-min resolution, byscreening for extreme events as well as events whose return periods are around the usual design return periods for stormwater systems. The European standard BS EN752:2008 recommends a design storm return period of 1 year for rural areas, 2 years for residential areas, 5 years for city centres without flooding checks, and up to 10 years for areas with underground railways (Butler et al., 2018). Finally, three events of different durations, referred as E_1, E_2 and E_3, were extracted from the historical data, with return periods ranging from 5 to 20 years. The highest event ever recorded in Trondheim from August 2007 was included, referred to as E_4. With a return period of more than 100 years, this extreme rainfall event was accompanied by flash floods and extreme flooding, triggering damage in the city. Table 2 presents those events and their estimated return periods.

As has been done in a previous study (Shuster et al., 2005), the catchment runoff descriptors used were the total outflow volume, made of the sum of the outflow volume and the flooding volume, and the peak runoff value. The peak flooding value was also extracted from the simulations output for each manhole. The flooding in SWMM is the overflow from manhole when the drainage pipe is surcharged. It is calculated when the pipe and manhole reached their full capacity (Rossman, 2015). The results for those indicators are presented both in raw values and in variation rates. The respective references for the evolution rates are given in the relevant sections.

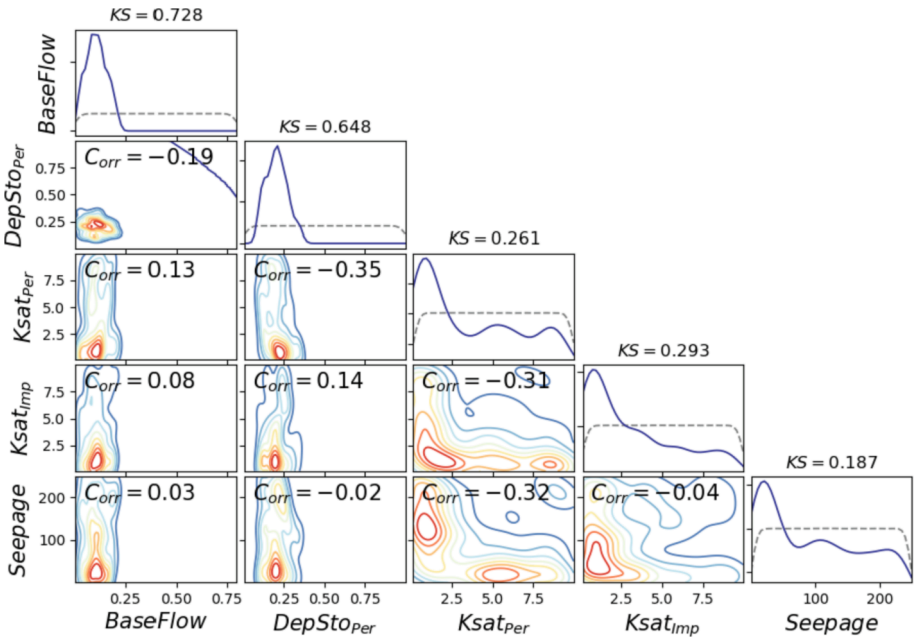

Fig. 4. Bivariate Kernel Density Estimation (KDE) plots (below diagonal) and univariate KDE plots (diagonal) of the most sensitive parameters of the SWMM model.

2.5.2. Urbanization

The catchment had an initial impervious rate, including roofs, sidewalks and road, of 27 %. Based on this reference scenario N_{ref}, seven urbanization scenarios were developed with different imperviousness rate ranging from 30 % to 90 %. Each scenario was named "N_X", where X was the target impervious rate. The scenarios were developed as follow: *i)* newly impervious areas were distributed in order to favour lowly impervious areas first and aim for homogenized imperviousness of each subcatchments but keeping the initial bias of scenario N_{ref} for each scenarios, *ii)* the maximum imperviousness rates was set to 95 %. For each urbanization scenario, the model parameters were updated using the impervious/pervious boundary defined during the calibration process. Scenarios N_{ref}, N_{60} and N_{90}, are studied more in detail in the later results.

2.5.3. LID implementation

The ten most impervious subcatchments in the current state of the Risvollan catchment, with an average of 51 % roofs, 37 % roads and 12 % pavements for the impervious areas, were the reference for the breakdown of impervious area in all scenarios.

The LID infrastructures were implemented by addition of unit components (with an area of 15 m^2 for green roofs and 100 m^2 for permeable pavements) until the total area of LID, obtained by the product of the target density and the available area, was reached in each target subcatchment.

Each LID implementation scenario was defined by the density of LID among the impervious area and the strategy of implementation of LID, i.e. the type of subcatchment where LID were implemented. Six implementation strategies were developed and are visible in Fig. 1: i) Homogeneous as a reference scenario, ii) left zone and iii) right zone to study the impact of intense implementation without favouring a distance to the outlet, iv) upstream, v) $downstream_1$ and vi) $downstream_2$ to study the influence of the distance to the outlet.

For the first scenario of homogenous LID spatial configurations, they were implemented in each subcatchment with the given density. For the following scenarios, the LID units were distributed randomly within the corresponding target subcatchments, until the target overall LID density was reached, or until the target zone was saturated in LID's, i.e., when all available pavements and roofs had been equipped with permeable pavements or green roofs, respectively.

2.5.4. Climate change

To account for the expected increase in heavy precipitation intensity, climate change factors were used in this study to compare the behaviour of the model for the different rainfall events and the different scenarios. Given the durations and the return periods of the chosen events, 2 factors were used in this study: 1, for the historical events without climate change, and 1.4, to study those same events accounting for climate change (Dyrrdal and Førland, 2019).

3. Results and discussion

3.1. Model parametrization

3.1.1. Calibration and validation results

It is a common practice to calibrate the impervious rate of subcatchments in SWMM models. The imperviousness degree is part of what Liong et al. (1991) calls non-traditional parameters. Contrary to the traditional parameters, i.e., infiltration parameters or depression storages, non-traditional parameters can technically be measured or interpreted from measures, but due to model limitations, relative errors and complex measurement procedures, they are often included in the calibration process and have relatively dominant effects. For example, Sangal & Bonema (1994) recommends the determination of the impervious rate to be the first step of the calibration, using a storm in which the rainfall intensity does not exceed the infiltration capacity of the pervious areas. More generally, with current automated calibration processes, this parameter is often included within the calibration parameter set, see for example (Hernes et al., 2020; Panos et al., 2018; Temprano et al., 2007), among many others. However, this method was not applicable here as the future urbanization scenarios would involve manipulations of the impervious rate.

The calibration resulted in KGE values ranging from 0.705 to 0.898 (Fig. 2) for the seven calibrated events. Kouchi et al. (2017) reports that a KGE $\geq$ 0.75 defines a good model performance, and KGE $\geq$ 0.5 defines a satisfactory model performance. This indicates a good to satisfactory calibration results. The model provides a satisfactory outflow timing and shape in most of the simulated events. However, the modelled peak values were underestimated for some events. The optimized parameter values are presented in Table 1. Fig. 3 presents the performance of the calibrated SWMM models on the six validation events. By comparing the

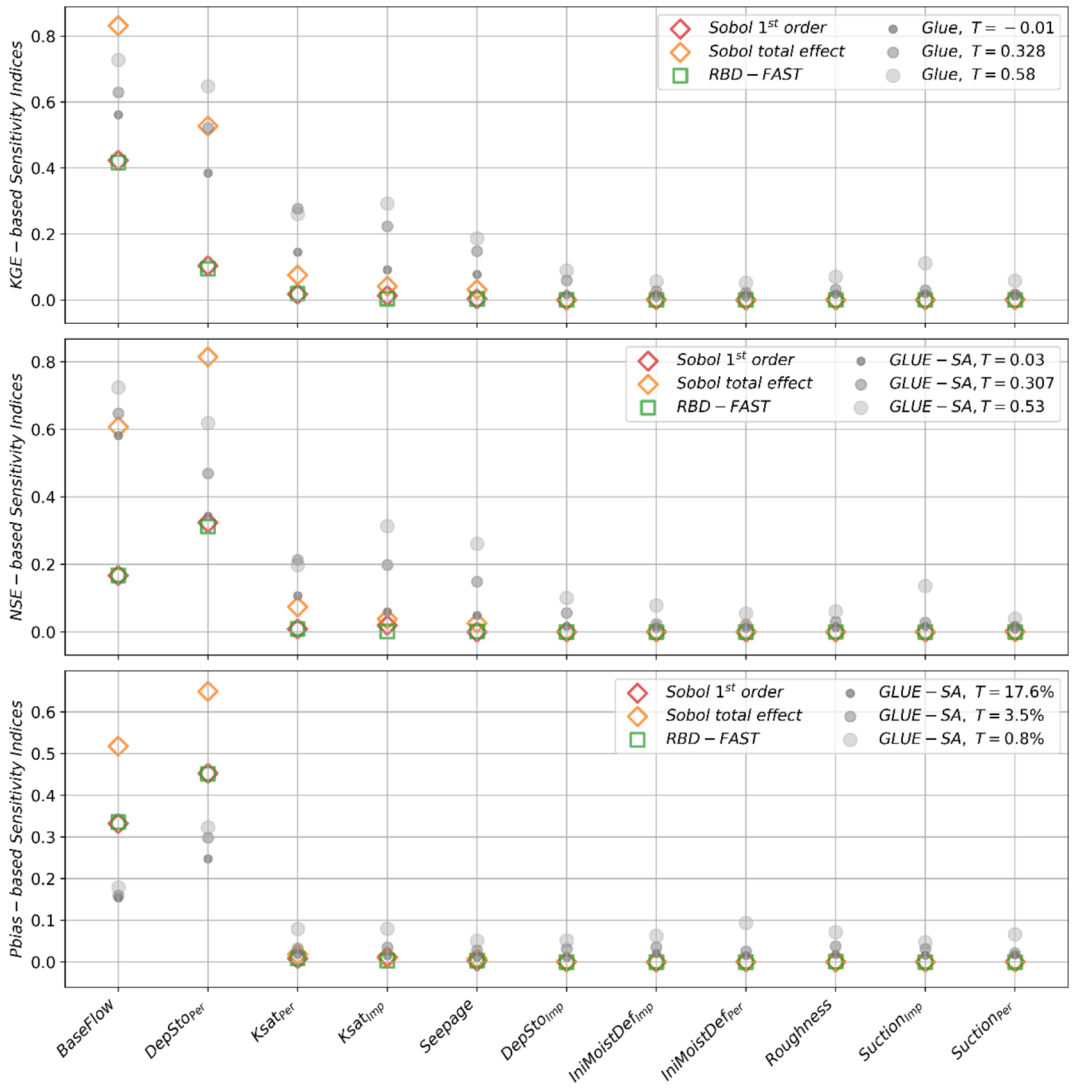

Fig. 5. Sensitivity measure of the Sobol, RDB_FAST method and the GLUE-based Sensitivity analysis (SA) using KGE, NSE and PBIAS as objective function. The order of the parameter is obtained from the raking according to RDB-FAST with KGE. Different thresholds were used for the GLUE-based SA to ensure that the filtered dataset contain 15%, 5% of 1% of the original dataset.

average of the ensemble with the observation, three events yielded simulation with satisfactory KGE values (KGE greater than 0.5). This means that for certain events (V_1, V_2 and V_4), the model performance was unsatisfactory, when only the mean of the ensemble is considered. However, the peak values of most of the validations events laid within the bounds of the ensemble, except for V_1. Hence, the SWMM model with the ensemble simulation is considered valuable for evaluating the effect of LID implementation on high flow values. Therefore, it was decided to apply the ensemble simulations for investigating scenarios of LID implementation.

3.1.2. Sensitivity analysis results

GLUE has been applied to the Risvollan model, as an assessment of uncertainty, to estimate the relative sensitivity of the parameters and screen the most behavioural ones.

After the filtering of the 65 000 parameter sets with KGE of 0.58 as a threshold value separating behavioural and non-behavioural parameters, 682 parameter sets were found to be behavioural, representing 1 % of the generated datasets. Fig. 4 presents the bivariate and the univariate kernel density (KDE) plots of the 5 most sensitive parameters of this SWMM model (BaseFlow, $DepSto_{Per}$, $Ksat_{Per}$, $Ksat_{Imp}$, Seepage). The two predominantly sensitive parameters, the baseflow and the depression storage in pervious area, highlight the characteristic of lowly urbanized catchment: there is a lot of uncertainty in the natural area behaviour and inflow going in the network. The hydraulic conductivities, and to a lesser extent the pipe seepage rate, absorb model irregularities and unmodelled hydrological processes in this model (e.g. interaction with groundwater) and smoothen the output.

The use of RBD-FAST method and Sobol 1st order and total effect indices (Fig. 5) led to a similar screening. However, the GLUE-based sensitivity is sensitive to the threshold used in terms of ranking. It should also be noted that the ranking depends on the objective function chosen. According to RBD-FAST and Sobol indices, the depression storage in pervious area is more sensitive than the baseflow in terms of NSE and Pbias. The ranking differ for NSE with the GLUE-based approach. Those results confirm that the GLUE methodology can be applied for screening behavioural and non-behavioural parameters if used carefully; despite the flexibility of the GLUE method, it does not allow to achieve similar ranking as the one achieved with the RBD-FAST or Sobol indices. The sizes of the filtered dataset can also influence the results, so the threshold should be carefully selected (Brunetti et al., 2016).

The review from Salvadore et al. (2015), that concluded that in many SWMM modelling studies, the most sensitive parameters are the

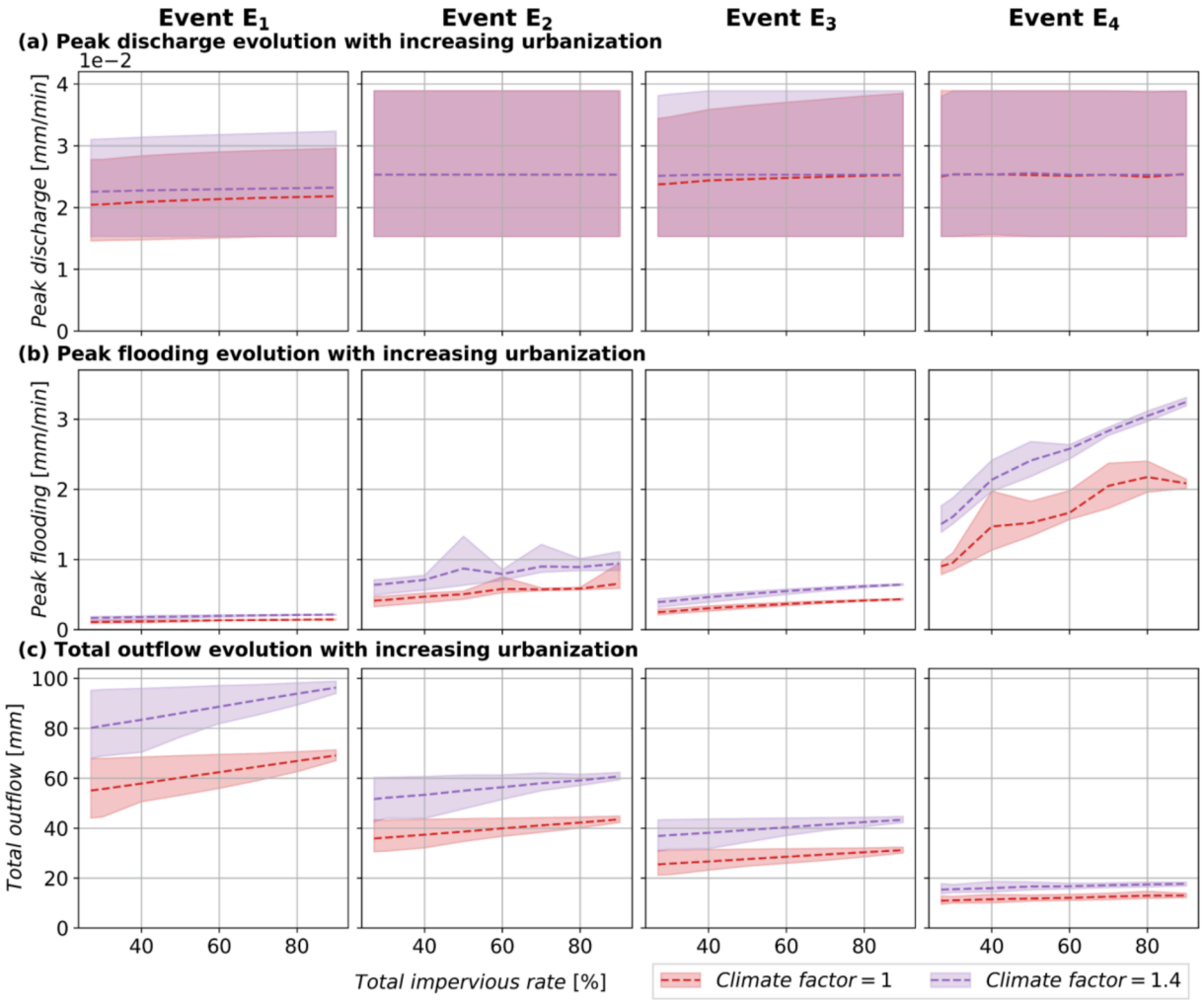

Fig. 6. Impacts of urbanization and climate change on urban runoff. The shaded areas represent the variabilities within the ensemble.

Manning's roughness coefficient of pipes and the impervious rate. In the current approach, due to the use of baseflow, the roughness had a lower influence. Due to the necessary hypothesis for LID implementation scenario, the impervious rate was not considered as a calibrated parameter. Krebs et al. (2013) found that for their model, the depression storage in impervious zones was the most sensitive parameter, similarly to the current study where it ranks 2nd.

The correlation between the most sensitive parameters is displayed on Fig. 4. With a maximum absolute value of 0.35, it appears that there is no strong correlation between any of the parameters, indicating an adequate independence of the parameters. This is reflected in total effect Sobol indices where the ranking remain unchanged from 1st order indices.

3.2. Scenarios exploration results

3.2.1. Effects of urbanization and climate change on current catchment

The results of the first simulations, aiming at evaluating the influence of urban growth and climate change on the study area, are presented in Fig. 6**.** Without accounting for climate change, the increase of urbanization already has a high impact on the flow indicators. For E_4, the peak flooding increase by 100 % and the total volume outflow by 20 % between the initial situation N_{ref} and the N_{90} urbanization scenario. The peak discharge stay stable since the maximum capacity of the outflow pipe is reached during the simulation. Hence, a stable peak discharge does not mean no effect. The total volume and the peak of flooding can still increase, e.g. for event E_4 with a climate factor of 1.4, with up to 62 % increase of total volume outflow and 260 % increase of peak flooding. While the linear increase of precipitation resulted in a linear increase in the total outflow volume, it appears that the increase of peak runoff is non-linear. E_2, E_3 and E_4 display an identical maximum peak value, around 0.038 mm, for several urbanization scenarios. This peak value most likely corresponds to the maximum outlet capacity of the network. Likewise, Ercolani et al. (2018) observed a non-linear peak reduction with respect to a catchment-scale green roof implementation. The authors attributed this non-linearity to drainage network being close to its maximum capacity.

The peak flooding values continue to increase, linearly for E_1, E_2 and E_3. Fig. 7 shows the spatial impact of an intense urbanization scenario (90 %) on the spatial flooding values at Risvollan. Intense precipitation events, especially E_4 and E_2, triggered flooding from different manholes at Risvollan under this intense urbanization scenario. It can be seen from Fig. 7 that some manholes experienced higher flooding values, especially at the downstream parts of Risvollan. Additionally, the results showed that flooding from sewer manholes is triggered by rainfall intensity and not by the rainfall amount. For instance, E_2 (return period = 2 y) caused more flooding than E_1 even though E_1 has more amount and higher return period (return period = 5 y), as summarized in Table 2.

3.2.2. Effects of homogenous LID

This section presents and discusses the results of homogenous LID implementation on all subcatchments. The variations of indicators induced by 100 % implementation of homogeneous LID for the different urbanization scenarios are presented in Fig. 8. Under the current climate

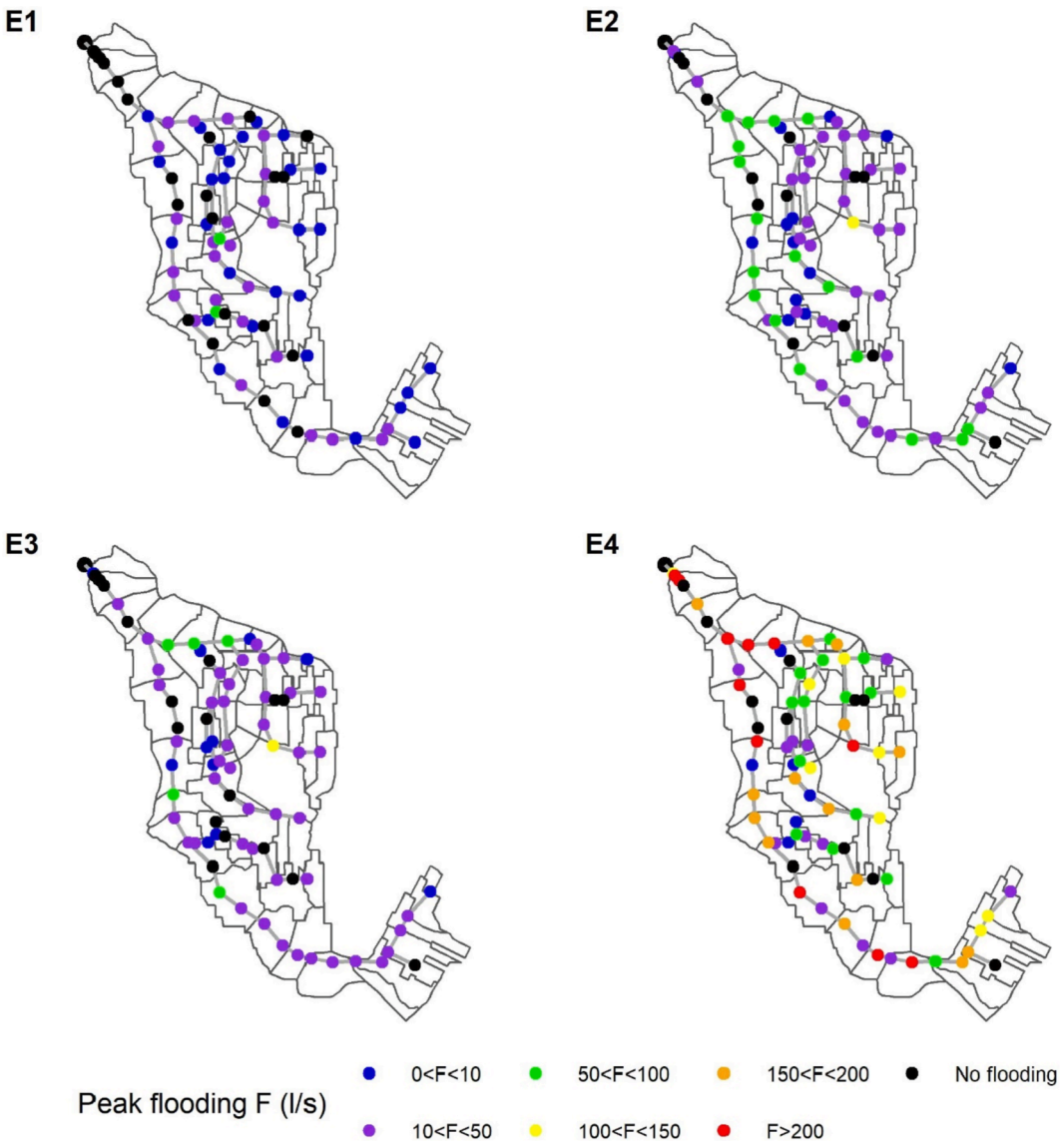

Fig. 7. Impacts of intense urbanization scenario (90 %) on peak flooding from manholes at Risvollan catchment without climate change (CF = 1).

for events E_1, E_2 and E_3, the peak discharge tends to decrease, its variation ranging from 0 to –22 %. It means that the more the city gets urbanized the more effective the LID gets. However, for E_2 and E_4, the maximum outlet flow, i.e. the capacity of the drainage network, is attained as shown in Fig. 8, obscuring the performance of the LID implementation. However, the evolution of peak flooding reflects the LID mitigation action, as it is very consistently reduced by large rates, between around 50 % for N_{90} and event E_2 and E_3.

Event E_4, the most extreme event out of the 4, with a return period of 100 years, yielded more erratic results than other events when it comes to peak reduction. This might be due the fact that the maximum pipe capacity is reached. In addition, the nature of this event, short and intense, triggers the complexity of the system and lead to more unforeseen peaks. The behaviour of the system was not investigated further regarding this matter; however, the peak flooding tends to decrease with presence of LID.

The results in Fig. 9 show the variation of peak discharge and flooding with the scenario N_{ref} No-LID as a reference. The scenario Homogeneous 100 % and No-LID are displayed. It shows for No-LID the increase of the indicators (except peak discharge when the pipe capacity is reached). The range corresponding to Homogeneous scenario showed that it is possible to compensate urbanization in most of the events (E_1, E_2 and E_3). However, when climate change is considered, it is not possible to come back to performance without climate factor and without urbanization. It is nonetheless possible to contain the effect of climate change with high urbanization.

The total outflow variation (Fig. 8**c**) appears to be almost linearly decreasing with LID density for all rainfall scenarios, with some outlier values appearing for E_4. At N_{90}, the reduction rate ranges between 12 and 46 %. When comparing these values to the pre-urbanization volumes (Fig. 9), it appears that it is not possible to compensate completely the imperviousness increase for all events and all model in the ensemble. However, the volume increase can be limited and often it can even decrease, e.g. for E_3 the volume vary between 5 and 45 % without LID and 10 to −20 % with LID, which evidently reduces the stress on the stormwater system. The range of the ensemble encompass model uncertainty and initial conditions variation. This approach shows the value of ensemble modelling with multiple events to cope with climate and condition variability.

When considering climate change, the effect on the total volume outflow of the system is the most prevalent, which is expected since the volume of the rainfall increases. On Fig. 8, the values of total volume and flooding are shifted according to the climate factor. The Peak discharge variation is only positive for E_1 since the maximum capacity of the

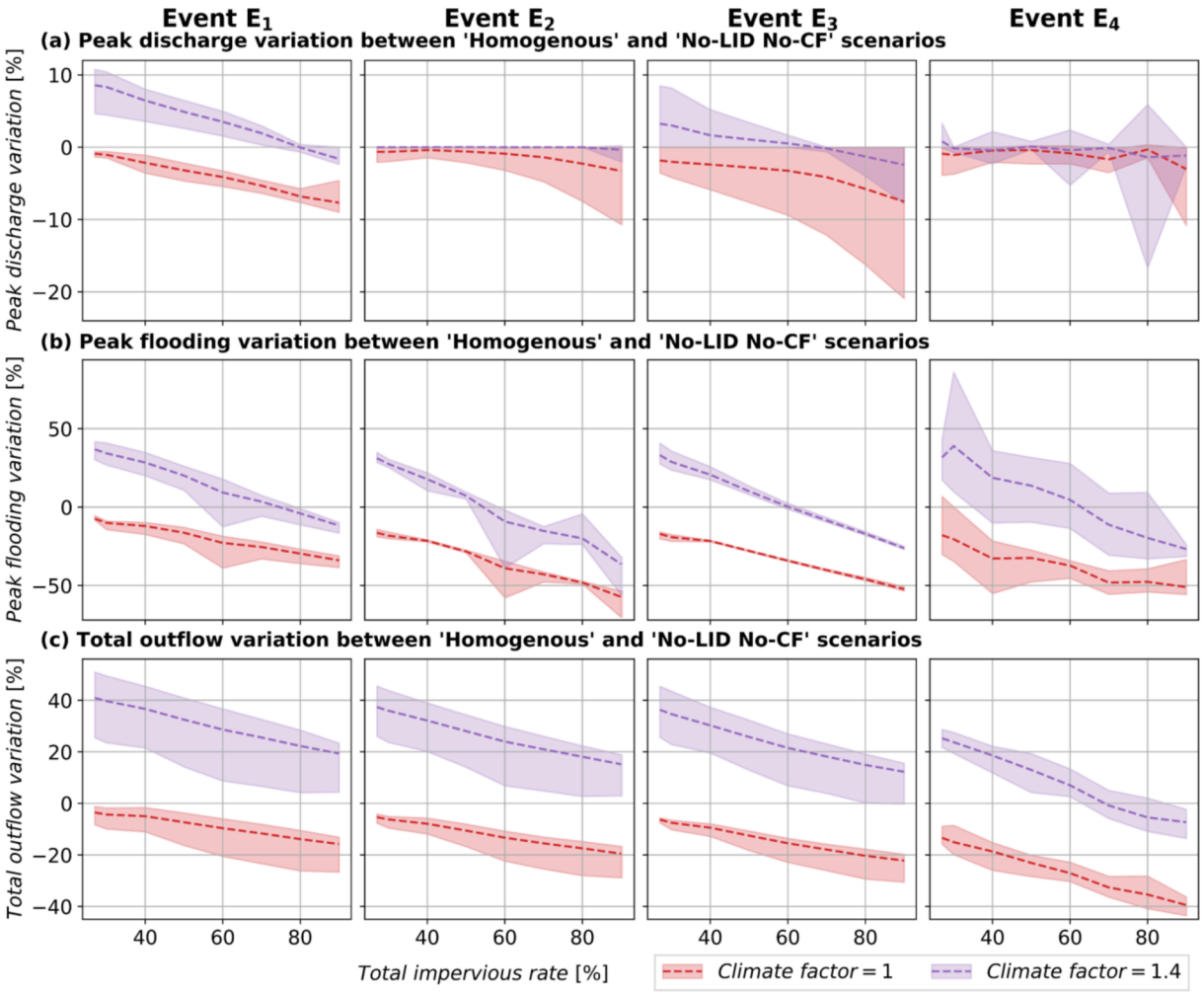

Fig. 8. Variation of performance induced by 100 % implementation of homogeneous LID depending on urbanization scenarios. The urbanization scenarios without LID are used as reference. Both current and future climate (Climate factor = 1.4) are displayed. The shaded areas represent the variabilities within the ensemble.

system was not reached. The LID implementation, occupying 100 % of available surfaces, cannot compensate both effect of urbanization and climate change (Fig. 9). However, it can compensate the effect of urbanization since the variation of total volume outflow stay stable with increasing urbanization when compared to N_{ref} without LID or climate factor.

Overall, homogenous LID implementation over the catchment was found to be an effective strategy to cope with increased urban runoff with increased urbanization and climate effects, for peak runoff, peak flooding, and total outflow volume. The LID implementation could partly compensate either urbanization or climate change, but can not fully compensate for the combination of the two.

3.2.3. *Influence of the spatial configurations of LID measures*

The variation of performance between the homogenous distribution and the five scenarios of spatial distribution of LID were evaluated. Fig. 10 and Fig. 11 presents the effects of LID implementation scenarios on peak discharge and total volume outflow variation, respectively, for three urbanization scenarios N_{ref}, N_{60} and N_{90}. In terms of total outflow volume and peak flooding, the left branch and right branch scenarios yielded similar results to those of the homogenous distribution. They were not found to be effective to reduce peak runoff. This indicates that there is no topographical or network difference that triggers a major behaviour difference in LID performance in those two zones. The results for peak discharge variation, indicate that the downstream scenarios can reach the same peak reduction levels as the homogenous LID with a smaller LID density, around 40 % for the first downstream scenario and 20 % for the second. In contrast, upstream implementation has little effect on the peak discharge downstream. However, when it comes to outflow volume, the different LID distributions perform the same as the homogenous distribution.

The spatial location of LID was found to influence the flooding from manholes. To demonstrate this finding, the six implementation scenarios were compared at a similar catchment scale LID density, which correspond to 100 % of LID in the target area of $downstream_2$, the limiting scenario, corresponding to 23 % of the full catchment (for homogeneous scenario). The other LID densities within their respective target area were: 48 % (left), 51 % (right), 47 % (upstream), and 45 % ($downstream_1$). These scenarios were investigated on event E_4 and urbanization N_{90} and by using one parameter set from the ensemble. These results are presented in Fig. 12. The homogenous configuration was found to be the least effective in reducing flooding peaks from manholes. Distributing LID at the upstream of the catchment resulted in flooding peak reductions in both the upstream and downstream manholes.

Even with the short concentration time of the Risvollan catchment, of around 10–15 min (Skaugen et al., 2020), the runoff from the upstream subcatchments has a lesser contribution to the peak flow due to the travelling processes, both overland and in the pipe network. Nevertheless, these results, along with the S-shape of the curves in Fig. 10, suggests that subcatchments close to a measurement point have higher influence on peaks. This implies the existence of critical subcatchments, located downstream and close to the outlet of interest, that

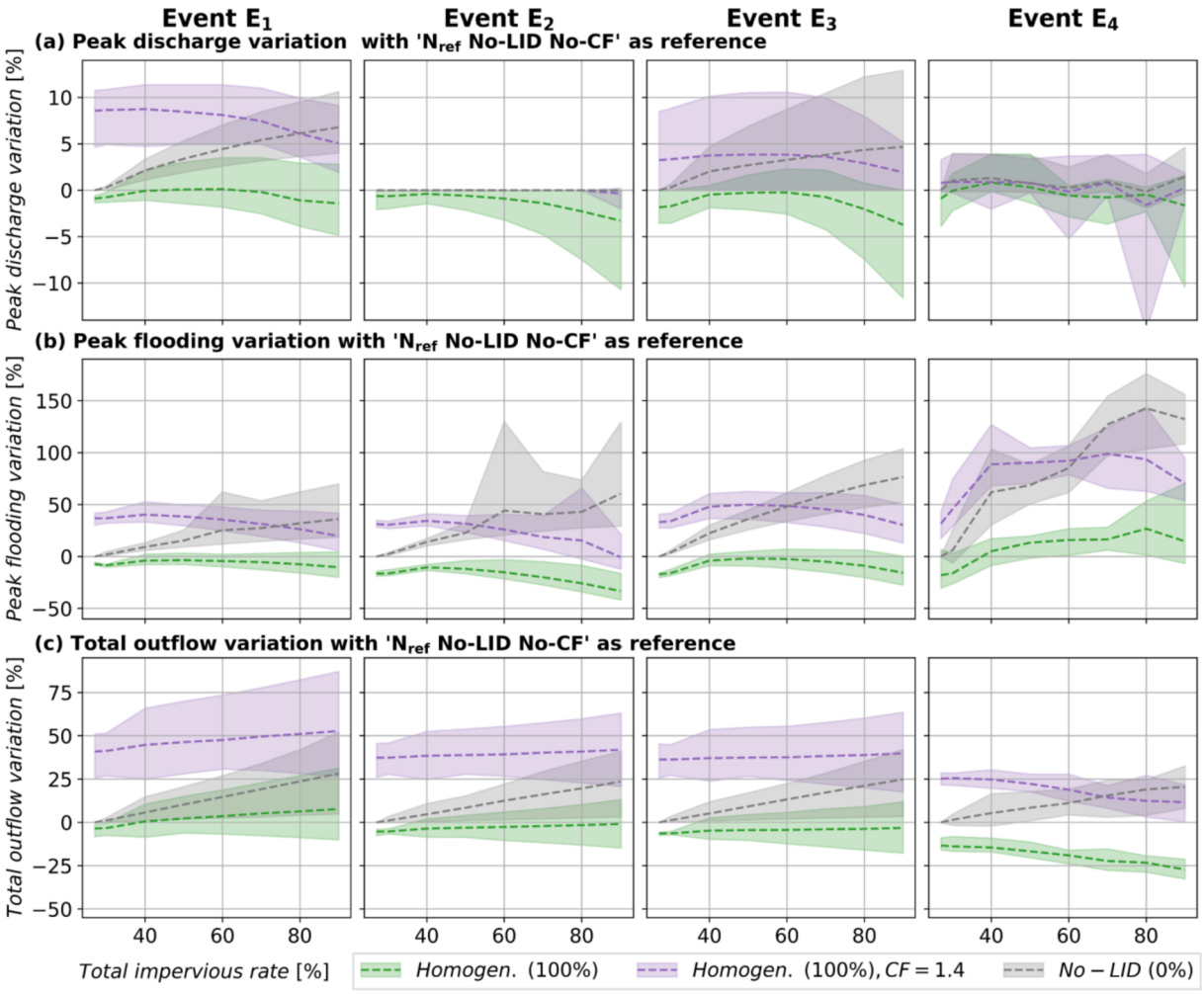

Fig. 9. Variation of performance depending on urbanization with and without LIDs. They are displayed for the homogeneous LID and the no-LID implementation scenarios. The initial urbanization (27%) without LID and climate factor (N_{ref} No-LID No-CF) is used as reference.

control most of the peak outflow, and that must be targeted to control it. Therefore, given a vulnerable outlet, if peak runoff is considered the most relevant indicator for the stress level put on the stormwater network, it seems possible to achieve the same performance as homogenous LID in a much more cost, time and resources-efficient way, by targeting the critical subcatchments situated downstream, near the vulnerable outlet. However, the performance in terms of total volume reduction is the same for all LID spatial distributions.

To compare these results with the findings of some studies around the same issues, Giacomoni & Joseph (2017) found placing LID at the downstream of the catchment to yield better peak reduction at the outlet, which is similar to the finding of this study. Hou et al. (2020), who developed an adaptive differential evolution algorithm to optimize the spatial priority scheme of various LID techniques, in Yichuan, China, recommended to place LID solutions near areas that are sensitive to flooding and pollution for achieving the most cost-effective stormwater management plan. Liang et al. (2020) found that peak flow reduction was most sensitive to the reduction of Directly Connected Impervious Areas (DCIA). Indeed, for a similar LID implementation, the results were better with less DCIA. Zellner et al. (2016) found that, with an increase in precipitation and in areas suitable for green infrastructures, implementation patterns that followed the flow paths and the accumulation of water also became more effective, which resonate with the results of this study. Ercolani et al. (2018) concluded that the urban system in the Metropolitan City of Milan, Italy, responded non-linearly to green roof density in terms of peak runoff reduction at the outfall. They related this non-linearity to the stormwater system being close to its conveyance capability. They studied a targeted green roof implementation that concentrated them on areas where conduits were prone to filling. This scenario showed a better performance than a homogenous implementation in terms of peak flow reduction at the outlet. This is coherent with the results of this study as downstream pipes are more vulnerable to filling as ending points of the entire network.

With respect to flooding, Zellner et al. (2016) found that spatially dispersed green infrastructure was more efficient to reduce flooding than clustered arrangements, which is different from the results observed in this study. It could be explained by the higher slopes in the current study. Especially clustered approaches were found to have more effective local effects.

3.3. Implications

This study examined the impacts of urbanization and climate change on the urban runoff response for the Risvollan catchment, as well as different LID implementation scenarios and their mitigating capacities. Our results highlight that climate change and urbanization put the current stormwater system under stress, and that LID infrastructures can participate in the mitigation of their effects. These results may constitute useful insight for municipalities.

Firstly, in this study, it appears that, depending on the target indicator to be reduced, the spatial distribution of LIDs can be an important factor for an effective design. Indeed, if the priority is to reduce the

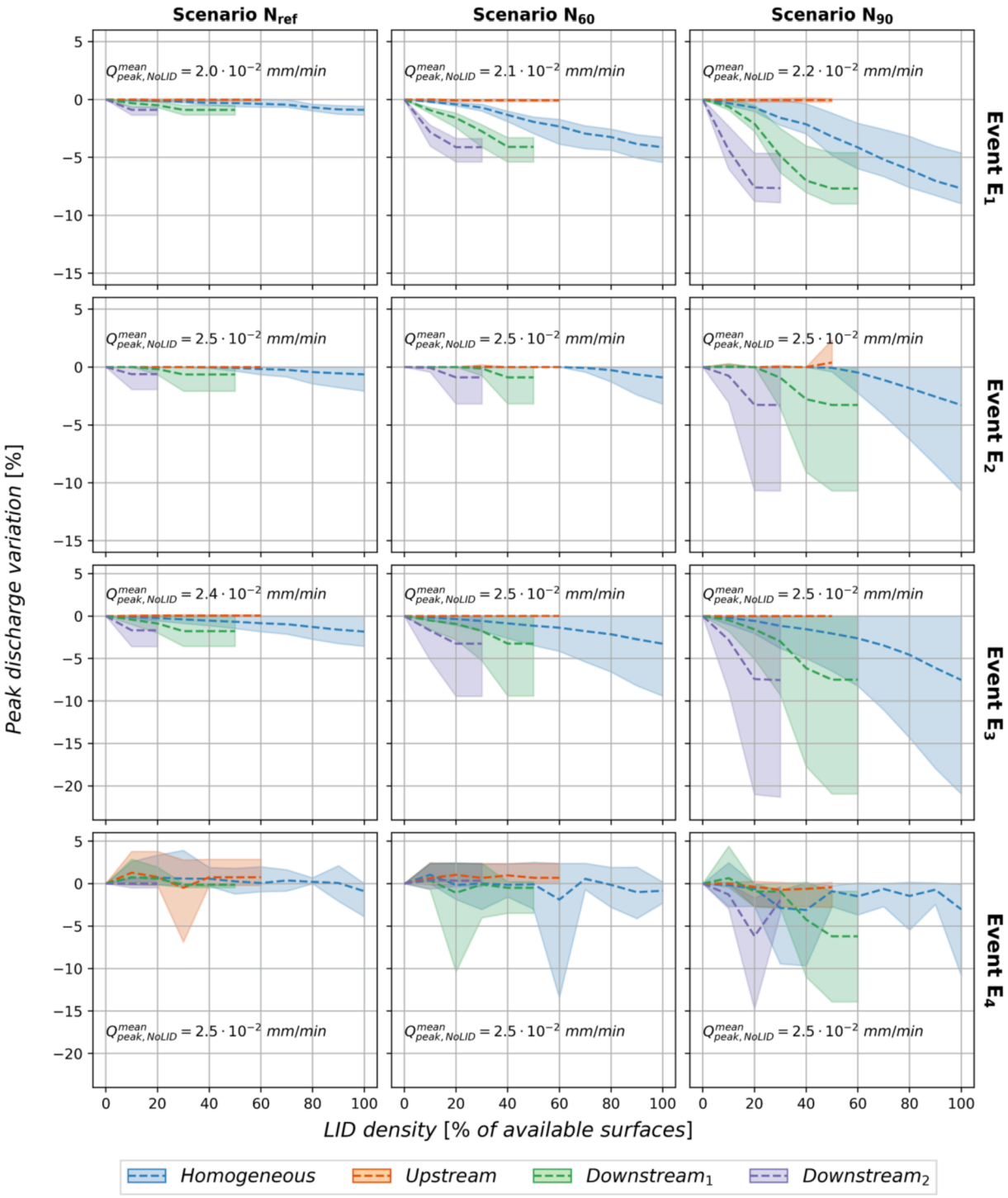

Fig. 10. Variation of peak discharge (%) at the outfall for different LID spatial distributions. The shaded areas represent the variabilities within the ensemble. The case Urbanization of Scenario N_0, N_{60} and N_{90} were displayed for events E_1, E_2, E_3 and E_4.

volume at the outfall of the catchment, the distribution of LID has little influence; whereas if the priority is the reduction of the outfall peak, it will be more resources and cost efficient to target the critical downstream subcatchments. This highlights an important aspect of green infrastructure implementation: the phasing of green infrastructure implementation. If the total outflow volume is not influenced by the strategy, the peak runoff in one location or local flooding is influenced by the implementation in its neighbourhood. Therefore, when it comes to prioritize implementation with limited resources, those results suggest that critical area should be directly prioritized. More precisely, the highly influential areas of the area of interest should be identified and prioritized. The use of model ensemble, despite showing similar trends in most of the case, shows the deep level of uncertainty associated with limited data and knowledge linked to a specific catchment. Secondly, the comparison of the LID performance for different rain events suggests that peak attenuation should be combined to return period to evaluate the bandwidth of LID performance. Indeed, the implemented LID infrastructure in this study was able to mitigate a 12 h event with a 20-years return period and a relatively low peak better than it could mitigate our 2 other events with a 5-year return period. Moreover, the

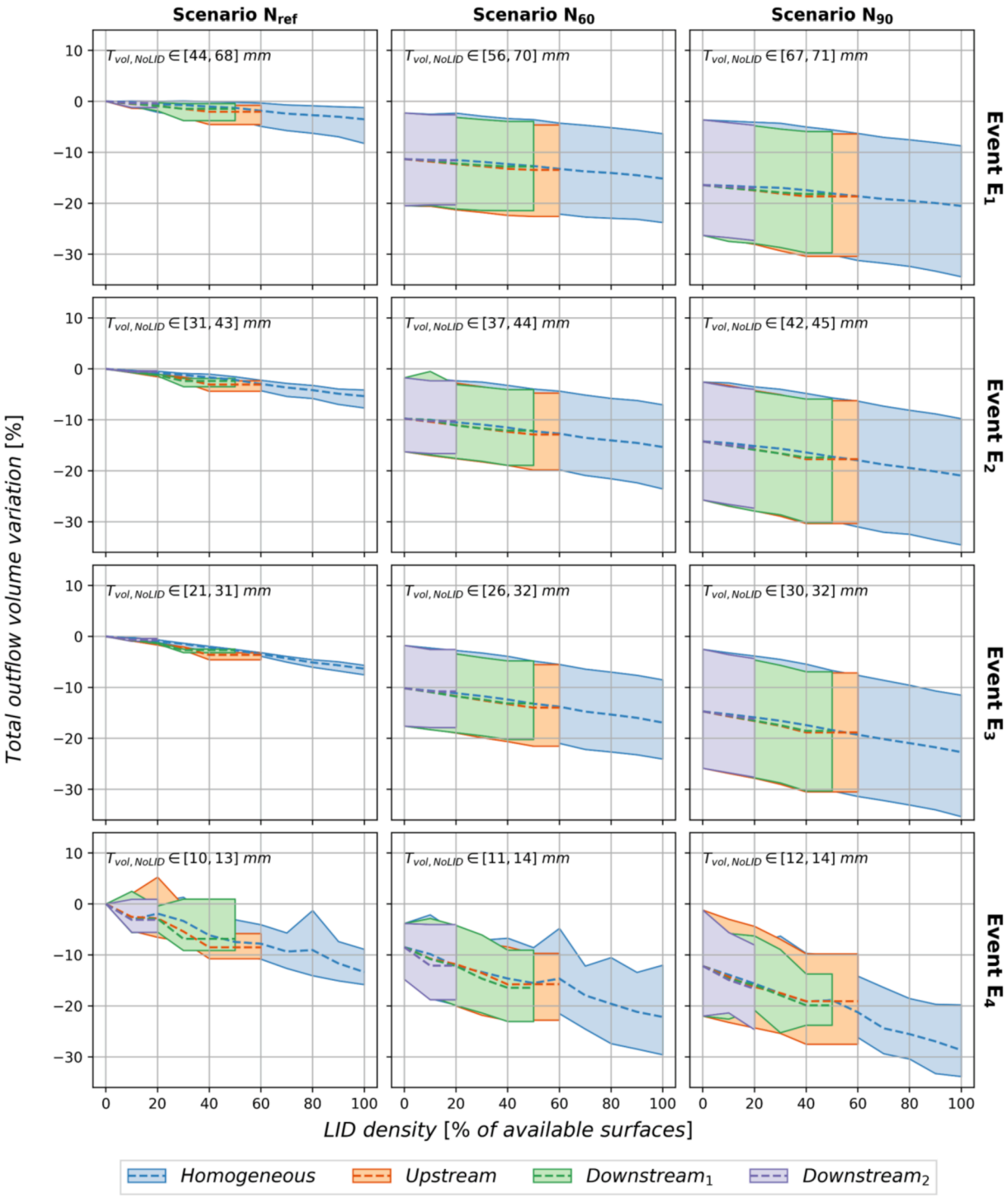

Fig. 11. Variation of total outflow volume (%) for different LID spatial distributions. The shaded areas represent the variabilities within the ensemble. The case Urbanization of Scenario N_0, N_{60} and N_{90} were displayed for events E_1, E_2, E_3 and E_4.

inclusion of a 100-year precipitation event in the rainfall scenarios provided erratic and inconclusive results, indicating the inadequacy of the method used for this case. This effect is interwined with the fact that our model was not calibrated for extreme events, and thus probably does not perform well in those cases. This highlights the need for further research to explore the behaviour of LID infrastructure under extreme events.

3.4. Limitations

Firstly, the rainfall input was event-based, which limits the ability to explore the behaviour of LID infrastructure under other types of rainfall than the four used here. For reference, Qin et al. (2013) described the performance difference of various LID infrastructures for different hydrograph shapes. Moreover, many studies have suggested more robust approaches to investigate LID performance, based on continuous rainfalls, i.e., long-term simulations (Stovin et al., 2017). Secondly, the calibration method used might have triggered unforeseen effects of the

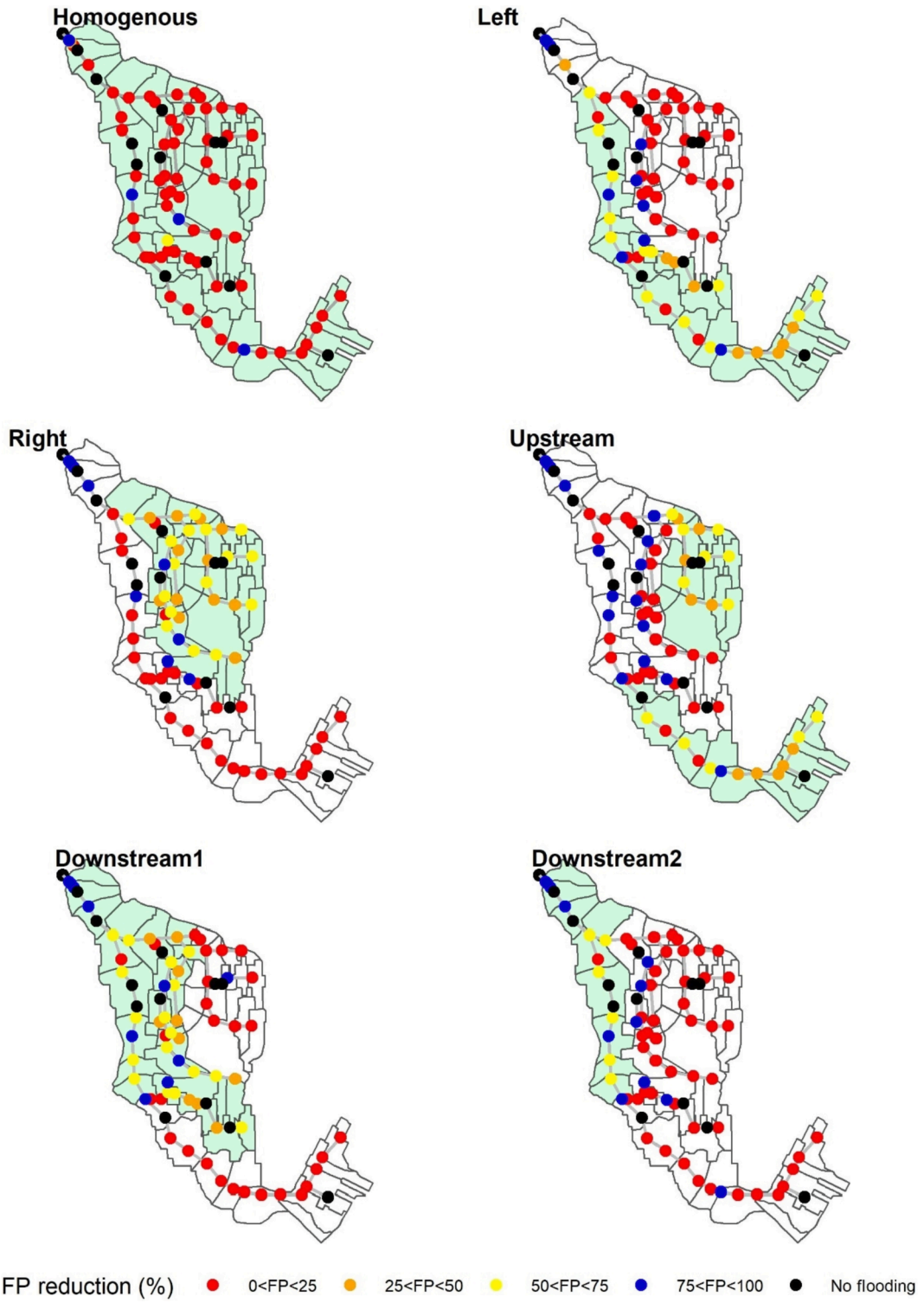

Fig. 12. Flooding peak reduction FP (%) for different LID spatial distributions in reference to full urbanization scenario and for E_4. The light green areas represent sub catchments with LID implementation.

adopted high pipe roughness. Further research might be needed to understand better the limitations of this method. Finally, this study used an aggregation of identical unit LID structures, whereas a more realistic study might need to precisely retrofit existing roofs and pavements.

4. Conclusion

This study implemented a SWMM model of the Risvollan catchment in Trondheim, Norway and investigated the impacts of various urbanization and climate change scenarios for 4 different rainfall events. Different LID densities were implemented with varying spatial distributions, and their performances in mitigating the effects of climate change and urbanization were explored.

The main results were as follows:

(i) The most sensitive parameters of the model were the baseflow of drainage pipes, the depression storage of pervious areas and the hydraulic conductivity.
(ii) Climate change and urbanization will deeply affect the catchment response to rainfall, up to 260 % increase in peak flooding and 75 % increase in volume flow.
(iii) The chosen LID infrastructure has demonstrated its ability to mitigate the effects of urbanization and climate change, with a varying performance depending, among other factors, on rainfall. However, they cannot completely compensate their effects.
(iv) The volume reduction performance of the LID infrastructures does not depend on spatial location, but the peak discharge at the outlet is more efficient if the LID structures are located downstream, close to the outfall. Therefore, given resources for a limited number of LID, the phasing of their implementation matters. LIDs located close to a vulnerable area should be implemented first.

Overall, urbanization and climate change put a high level of stress on the stormwater system, and LID techniques can help to mitigate that stress. Their spatial distribution may be a significant criterion to be accounted for when aiming for effective design, depending on the local stakes and particularities.

CRediT authorship contribution statement

Ninon Le Floch: Conceptualization, Methodology. **Vincent Pons:** Conceptualization, Methodology. **Elhadi Mohsen Hassan Abdalla:** Conceptualization, Methodology. **Knut Alfredsen:** Conceptualization, Methodology.

Declaration of Competing Interest

Financial support: This research has been supported by the Norges Forskningsråd (grant no. 237859/030).

References

Abdalla, E.M.H., Selseth, I., Muthanna, T.M., Helness, H., Alfredsen, K., Gaarden, T., Sivertsen, E., 2021. Hydrological performance of lined permeable pavements in Norway. Blue-Green Syst. 3 (1), 107–118. https://doi.org/10.2166/bgs.2021.009.
Bengtsson, L., Grahn, L., Olsson, J., 2005. Hydrological function of a thin extensive green roof in southern Sweden. Nord. Hydrol. 36 (3), 259–268. https://doi.org/10.2166/nh.2005.0019.
Beven, K., Binley, A., 1992. The future of distributed models: Model calibration and uncertainty prediction. Hydrol. Process. 6 (3), 279–298. https://doi.org/10.1002/hyp.3360060305.
Braswell, A.S., Winston, R.J., Hunt, W.F., 2018. Hydrologic and water quality performance of permeable pavement with internal water storage over a clay soil in Durham, North Carolina. J. Environ. Manage. 224, 277–287. https://doi.org/10.1016/j.jenvman.2018.07.040.
Brunetti, G., Šimůnek, J., Piro, P., 2016. A comprehensive numerical analysis of the hydraulic behavior of a permeable pavement. J. Hydrol. 540, 1146–1161.
Butler, D., Digman, C., Makropoulos, C., Davies, J.W., 2018. Urban Drainage. CRC Press.
Drake, J.A.P., Bradford, A., Marsalek, J., 2013. Review of environmental performance of permeable pavement systems: state of the knowledge. Water Qual. Res. J. Can. 48 (3), 203–222. https://doi.org/10.2166/wqrjc.2013.055.
Dreelin, E.A., Fowler, L., Carroll, C.R., 2006. A test of porous pavement effectiveness on clay soils during natural storm events. Water Res. 40 (4), 799–805. https://doi.org/10.1016/j.watres.2005.12.002.
Dunnett, N., Kingsbury, N., 2004. Planting Green Roofs and Living Walls. Timber Press, Cambridge, UK.
Dyrrdal, A. V., & Førland, E. J. (2019). *Klimapåslag for korttidsnedbør: Anbefalte verdier for Norge. 5/2019*, Norsk klimaservicesenter. https://cms.met.no/site/2/klimaservicesenteret/rapporter-og-publikasjoner/_attachment/14869?_ts=16b02bdea3a.
Eckart, K., McPhee, Z., Bolisetti, T., 2017. Performance and implementation of low impact development – A review. *Sci. Total Environ.* 607-608, 413–432.
Ercolani, G., Chiaradia, E.A., Gandolfi, C., Castelli, F., Masseroni, D., 2018. Evaluating performances of green roofs for stormwater runoff mitigation in a high flood risk urban catchment. J. Hydrol. 566 (September), 830–845. https://doi.org/10.1016/j.jhydrol.2018.09.050.
Fassman, E.A., Blackbourn, S., 2010. Urban runoff mitigation by a permeable pavement system over impermeable soils. J. Hydrol. Eng. 15 (6), 475–485. https://doi.org/10.1061/(asce)he.1943-5584.0000238.
Giacomoni, M.H., Joseph, J., 2017. Multi-objective evolutionary optimization and monte carlo simulation for placement of low impact development in the catchment scale. J. Water Resour. Plan. Manage. 143 (9) https://doi.org/10.1061/(ASCE)WR.1943-5452.0000812.
Gupta, H.V., Kling, H., Yilmaz, K.K., Martinez, G.F., 2009. Decomposition of the mean squared error and NSE performance criteria: Implications for improving hydrological modelling. J. Hydrol. 377 (1–2), 80–91. https://doi.org/10.1016/j.jhydrol.2009.08.003.
Hailegeorgis, T.T., Alfredsen, K., 2018. High spatial–temporal resolution and integrated surface and subsurface precipitation-runoff modelling for a small stormwater catchment. J. Hydrol. 557, 613–630. https://doi.org/10.1016/j.jhydrol.2017.12.054.
Hamouz, V., Møller-Pedersen, P., Muthanna, T.M., 2020. Modelling runoff reduction through implementation of green and grey roofs in urban catchments using PCSWMM. Urban Water J. 17 (9), 813–826. https://doi.org/10.1080/1573062X.2020.1828500.
Han, J., He, S., 2021. Urban flooding events pose risks of virus spread during the novel coronavirus (COVID-19) pandemic. Sci. Total Environ. 755, 142491 https://doi.org/10.1016/j.scitotenv.2020.142491.
Hernes, R.R., Gragne, A.S., Abdalla, E.M.H., Braskerud, B.C., Alfredsen, K., Muthanna, T. M., 2020. Assessing the effects of four SUDS scenarios on combined sewer overflows in Oslo, Norway: evaluating the low-impact development module of the Mike Urban model. Hydrol. Res. 51 (6), 1437–1454. https://doi.org/10.2166/nh.2020.070.
Hou, J., Zhu, M., Wang, Y., Sun, S., 2020. Optimal spatial priority scheme of urban LID-BMPs under different investment periods. Landscape Urban Plann. 202 (539), 103858 https://doi.org/10.1016/j.landurbplan.2020.103858.
Johannessen, B.G., Muthanna, T.M., Braskerud, B.C., 2018. Detention and retention behavior of four extensive green roofs in three Nordic climate zones. Water (Switzerland) 10 (6), 671. https://doi.org/10.3390/w10060671.
Johannessen, B.G., Hamouz, V., Gragne, A.S., Muthanna, T.M., 2019. The transferability of SWMM model parameters between green roofs with similar build-up. J. Hydrol. 569, 816–828. https://doi.org/10.1016/j.jhydrol.2019.01.004.
Kouchi, D.H., Esmaili, K., Faridhosseini, A., Sanaeinejad, S.H., Khalili, D., Abbaspour, K. C., 2017. Sensitivity of calibrated parameters and water resource estimates on different objective functions and optimization algorithms. Water 9 (6). https://doi.org/10.3390/w9060384.
Krebs, G., Kokkonen, T., Valtanen, M., Koivusalo, H., Setälä, H., 2013. A high resolution application of a stormwater management model (SWMM) using genetic parameter optimization. Urban Water J. 10 (6), 394–410. https://doi.org/10.1080/1573062x.2012.739631.
Krebs, G., Kuoppamäki, K., Kokkonen, T., Koivusalo, H., 2016. Simulation of green roof test bed runoff. Hydrol. Process. 30 (2), 250–262. https://doi.org/10.1002/hyp.10605.
Leutnant, D., Döring, A., Uhl, M., 2019. swmmr - an R package to interface SWMM. Urban Water J. 16 (1), 68–76.
Liang, C., Zhang, X., Xia, J., Xu, J., She, D., 2020. The effect of sponge city construction for reducing directly connected impervious areas on hydrological responses at the urban catchment scale. Water (Switzerland) 12 (4). https://doi.org/10.3390/W12041163.
Liong, S.Y., Chan, W.T., Lum, L.H., 1991. Knowledge-based system for SWMM runoff component calibration. J. Water Resour. Plann. Manage. 117 (5), 507–524. https://doi.org/10.1061/(ASCE)0733-9496(1991)117:5(507).
Mullen, K.M., Ardia, D., Gil, D.L., Windover, D., Cline, J., 2011. DEoptim: an R package for global optimization by differential evolution. J. Stat. Softw. https://doi.org/10.18637/jss.v040.i06.
Palla, A., Gnecco, I., 2015. Hydrologic modeling of low impact development systems at the urban catchment scale. J. Hydrol. 528, 361–368. https://doi.org/10.1016/j.jhydrol.2015.06.050.
Palla, A., Sansalone, J.J., Gnecco, I., Lanza, L.G., 2011. Storm water infiltration in a monitored green roof for hydrologic restoration. Water Sci. Technol. 64 (3), 766–773. https://doi.org/10.2166/wst.2011.171.
Panos, C.L., Hogue, T.S., Gilliom, R.L., Mccray, J.E., 2018. High-resolution modeling of infill development impact on stormwater dynamics in Denver, Colorado. J. Sustain. Water Built Environ. 4 (4), 4018009. https://doi.org/10.1061/jswbay.0000863.
Peng, Z., Stovin, V., 2017. Independent validation of the SWMM green roof module. J. Hydrol. Eng. 22 (9), 04017037. https://doi.org/10.1061/(ASCE)HE.1943-5584.0001558.
Qin, Hua-peng, Li, Zhuo-xi, Fu, Guangtao, 2013. The effects of low impact development on urban flooding under different rainfall characteristics. Journal of Environmental Management 129, 577–585. https://doi.org/10.1016/j.jenvman.2013.08.026.
Rossman, L.A., 2015. STORM WATER MANAGEMENT MODEL USER'S MANUAL Version 5.1. National Risk Management Laboratory office of Research and Development. United States Environmental Protection Agency, Cincinnati, Ohio.
Saltelli, A., Ratto, M., Andres, T., Campolongo, F., Cariboni, J., Gatelli, D., Saisana, M., Tarantola, S., 2007. Global sensitivity analysis. Primer. https://doi.org/10.1002/9780470725184.
Salvadore, E., Bronders, J., Batelaan, O., 2015. Hydrological modelling of urbanized catchments: a review and future directions. J. Hydrol. 529, 62–81. https://doi.org/10.1016/j.jhydrol.2015.06.028.
Sangal, S., Bonema, S.R., 1994. A methodology for calibrating SWMM models. *J. Water Manage. Model.* https://doi.org/10.14796/jwmm.r176-24.
Semadeni-Davies, A., Hernebring, C., Svensson, G., Gustafsson, L.G., 2008. The impacts of climate change and urbanisation on drainage in Helsingborg, Sweden: combined sewer system. J. Hydrol. 350 (1–2), 100–113. https://doi.org/10.1016/j.jhydrol.2007.05.028.

Shuster, W.D., Bonta, J., Thurston, H., Warnemuende, E., Smith, D.R., 2005. Impacts of impervious surface on watershed hydrology: a review. Urban Water J. 2 (4), 263–275. https://doi.org/10.1080/15730620500386529.

Skaugen, T., Lawrence, D., Ortega, R.Z., 2020. A parameter parsimonious approach for catchment scale urban hydrology – Which processes are important? J. Hydrol. X 8 (July), 100060. https://doi.org/10.1016/j.hydroa.2020.100060.

Skougaard Kaspersen, P., Høegh Ravn, N., Arnbjerg-Nielsen, K., Madsen, H., Drews, M., 2017. Comparison of the impacts of urban development and climate change on exposing European cities to pluvial flooding. Hydrol. Earth Syst. Sci. 21 (8), 4131–4147. https://doi.org/10.5194/hess-21-4131-2017.

Sobol, I.M., 2001. Global sensitivity indices for nonlinear mathematical models and their Monte Carlo estimates. Math. Comput. Simul. 55 (1-3), 271–280.

Sorteberg, A., Lawrence, D., Dyrrdal, A.V., Mayer, S., Engeland, K., 2018. Climatic changes in short duration extreme precipitation and rapid onset flooding - implications for design values. NCCS 1.

Storn, R., Price, K., 1997. Differential evolution - A simple and efficient heuristic for global optimization over continuous spaces. J. Global Optim. 11 (4), 341–359. https://doi.org/10.1023/A:1008202821328.

Stovin, V., 2010. The potential of green roofs to manage urban stormwater. Water Environ. J. 24 (3), 192–199. https://doi.org/10.1111/j.1747-6593.2009.00174.x.

Stovin, V., Vesuviano, G., Kasmin, H., 2012. The hydrological performance of a green roof test bed under UK climatic conditions. J. Hydrol. 414–415, 148–161. https://doi.org/10.1016/j.jhydrol.2011.10.022.

Stovin, V., Vesuviano, G., De-Ville, S., 2017. Defining green roof detention performance. Urban Water J. 14 (6), 574–588. https://doi.org/10.1080/1573062X.2015.1049279.

Støvring, J., Dam, T., Jensen, M.B., 2018. Hydraulic performance of lined permeable pavement systems in the built environment. Water (Switzerland) 10 (5), 587. https://doi.org/10.3390/w10050587.

Tarantola, S., Gatelli, D., Mara, T.A., 2006. Random balance designs for the estimation of first order global sensitivity indices. Reliab. Eng. Syst. Saf. 91 (6), 717–727. https://doi.org/10.1016/j.ress.2005.06.003.

Temprano, J., Arango, Ó., Cagiao, J., Suárez, J., Tejero, I., 2007. Stormwater quality calibration by SWMM: a case study in Northern Spain. Water SA 32 (1). https://doi.org/10.4314/wsa.v32i1.5240.

Winston, R.J., Dorsey, J.D., Smolek, A.P., Hunt, W.F., 2018. Hydrologic performance of four permeable pavement systems constructed over low-permeability soils in Northeast Ohio. J. Hydrol. Eng. 23 (4), 04018007. https://doi.org/10.1061/(asce)he.1943-5584.0001627.

Yao, L., Wu, Z., Wang, Y., Sun, S., Wei, W., Xu, Y., 2020. Does the spatial location of green roofs affects runoff mitigation in small urbanized catchments? J. Environ. Manage. 268 (October), 110707 https://doi.org/10.1016/j.jenvman.2020.110707.

Zellner, M., Massey, D., Minor, E., Gonzalez-Meler, M., 2016. Exploring the effects of green infrastructure placement on neighborhood-level flooding via spatially explicit simulations. Comput. Environ. Urban Syst. 59, 116–128. https://doi.org/10.1016/j.compenvurbsys.2016.04.008.

Zhou, Q., Mikkelsen, P.S., Halsnæs, K., Arnbjerg-Nielsen, K., 2012. Framework for economic pluvial flood risk assessment considering climate change effects and adaptation benefits. J. Hydrol. 414–415, 539–549. https://doi.org/10.1016/j.jhydrol.2011.11.031.